ACS Sustainable Chemistry & Engineering

Research Article

pubs.acs.org/journal/ascecg

Efficient Photoelectrochemical Hydrogen Generation from Water Using a Robust Photocathode Formed by CdTe QDs and Nickel Ion

Yuming Dong,*,† Ruixian Wu,† Pingping Jiang, Guangli Wang, Yanmei Chen, Xiuming Wu, and Chi Zhang

Key Laboratory of Food Colloids and Biotechnology (Ministry of Education of China), School of Chemical and Material Engineering, Jiangnan University, Wuxi 214122, People's Republic of China

Supporting Information

ABSTRACT: Design of a novel sensitized NiO photocathode with wide visible light absorption and good stability is of great significance for photoelectrochemical hydrogen evolution. Inspired by recent reports on novel photocatalytic hydrogen evolution systems based on semiconductor quantum dots (QDs) and earth-abundant inorganic metal ion, we demonstrate the fabrication of an effective and stable photocathode by CdTe QDs and nickel ion. This photocathode showed good activity and stability for photocatalytic H_2 evolution (10.38 μmol) at a low overpotential of 92 mV, in which the Faradaic efficiency was almost 100% under visible light irradiation for 30 000 s. Characterized by X-ray photoelectron spectroscopy, X-ray powder diffraction and high-resolution transmission electron microscopy, the active site of photocathode in producing hydrogen by water splitting was found to be NiS@QDs. Then a possible mechanism of NiS@QDs for photoelectrochemical hydrogen evolution was proposed.

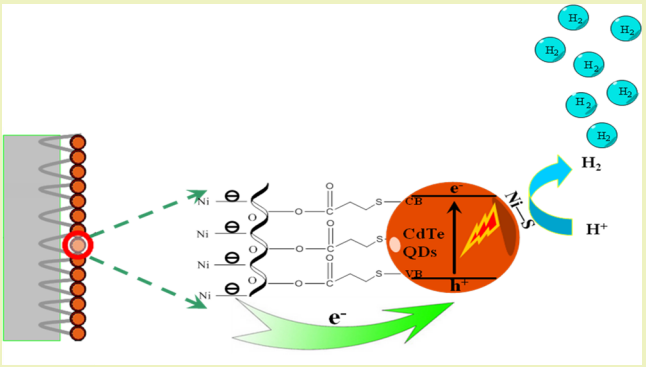

KEYWORDS: *Quantum dots, Photocatalysis, Water splitting, Hydrogen evolution, Solar energy*

INTRODUCTION

Solar driven splitting of water into molecular hydrogen and oxygen represents one of the most promising approaches to the use of solar energy. It is still greatly challenging to develop a robust, inexpensive, and efficient solar water splitting system.[1,2] Photoelectrochemical (PEC) cells are useful devices designed for the chemical process of generating hydrogen via electrolysis of water under irradiation of sunlight. In general, PEC devices are composed of two different photoelectrodes, photocathode and photoanode, where reduction and oxidation of water occur with response to sunlight. This provides an ideal and feasible scheme for solar driven overall water splitting.[3,4] As to the photocathode, although intensive research progresses have been made,[5−13] to develop efficient and stable photocathodes that can successfully serve practical needs is still of great challenge and significance.

Nickel oxide is an intrinsic nonstoichiometric *p*-type semiconductor with wide bandgap (E_g = 3.6−4.0 eV), exhibiting good thermal and chemical stability. In dye sensitized solar cells, NiO as a hole conductor sensitized by dye molecules is widely used.[14] In the PEC water splitting for hydrogen generation, several dye-sensitized NiO photocathodes were reported.[12,13,15] Limited by the nature of organic dye, the wavelength range of excitation light is narrow and the overall conversion efficiency of solar energy is low. In addition, organic dye is easily oxidized and dye sensitized NiO photocathode is unstable in the presence of oxygen. Therefore, design of a novel sensitized NiO photocathode with wide visible light absorption range and good stability is of great significance for PEC hydrogen evolution.

Compared with organic dye, quantum dots (QDs) have attracted widespread interest because their quantum confinement effect and broad and intense absorption spectra in the visible light region such as cadmium telluride (CdTe).[16,17] Recently, Richard Eisenberg's and Li-Zhu Wu's Group[16,18−22] respectively reported their novel photocatalytic hydrogen evolution systems based on semiconductor QDs and inorganic metal ion (Ni^{2+} or Co^{2+}). Up to now, these earth-abundant inorganic photocatalysts are among the most attractive visible-light-driven hydrogen evolution catalysts for their unprecedented activity and stability. However, one concern regarding these works, as well as many other studies that have been conducted for the light-driven generation of H_2,[23,24] is the need for a sacrificial electron donor. As known, nonsacrificial overall water splitting is the eventual goal in this field, and the performance of these QDs decides that they cannot make water oxidation for providing electron. Hence, it is highly desired to

Received: May 21, 2015
Revised: July 27, 2015
Published: September 9, 2015

ACS Publications © 2015 American Chemical Society

DOI: 10.1021/acssuschemeng.5b00450
ACS Sustainable Chem. Eng. 2015, 3, 2429−2434

propose a novel strategy for making best use of these remarkable photocatalysts in water splitting.

Therefore, a combination of QDs-sensitized NiO photocathode and inorganic metal ion could be considered as a good way to visible-light-driven hydrogen evolution. Inspired by these progresses, this work reports on the fabrication of an effective and stable photocathode based on NiO/QDs and nickel ion. First, this photocathode as a working electrode has shown predominant activity and stability. Then, the factors that played the catalytic role in the experiment were explored. The absence of any of the components, QDs, Ni^{2+} ions, overpotential, or visible light, resulted in no or low H_2 evolution. A possible photocatalytic mechanism of NiS@QDs on the improvement of the photoelectrocatalysis hydrogen evolution was proposed.

EXPERIMENTAL SECTION

Fabrication of NiO/QDs Photocathode. NiO films were fabricated by a hydrothermal method on ITO substrates and sintered at 300 °C. The CdTe QDs stabilized by 3-mercaptopropionic acid (MPA) employed in this study were synthesized following an earlier published report.[17] These MPA-CdTe QDs were deposited onto NiO films which was used as a *p*-type semiconductor fundus by immersing the film in an aqueous MPA-CdTe QDs solution (pH = 10) for 12 h. After the NiO film was soaked in the QDs solution, the film turns yellow in color, confirming the attachment of the MPA-CdTe QDs.

Characterization. UV−vis absorption spectra were recorded with a Shimadzu TU-1901 spectrophotometer. Scanning electron microscopy (SEM) was performed on an S-4800 (Hitachi, Japan) and operated at an accelerating voltage of 1.0 kV. X-ray diffraction (XRD) patterns were taken on a Bruker D8 Focus under Cu Kα radiation at (λ = 1.5406 Å). The amount of H_2 was characterized by GC analysis, which was performed with a FULI GC9790 using a 5 Å molecular sieve column and a thermal conductivity detector. The X-ray photoelectron spectroscopy (XPS) measurements were performed on an PHI 5000 VersaProbe (UIVAC-PHI, Japan) spectrophotometer. The high-resolution transmission electron microscopy (HRTEM) image was collected on a JEM-2100 transmission electron microscope (JEOL, Japan).

Measurement of Photoelectrochemical Properties and Hydrogen Generation from PEC. All of photoelectrochemical properties were probed using the three-electrode system that was linked with a CHI600 electrochemical workstation (Shanghai, China) and a 300 W xenon lamp with light filter (>400 nm) as the visible light source. The working electrode was a NiO electrode or NiO/QDs electrode (1.0 cm × 1.0 cm active area on 1.0 cm × 2.5 cm ITO). An aqueous Ag/AgCl electrode in 3 M KCl and a Pt wire were employed as the reference and counter electrode, respectively. The three-electrode system for H_2 evolution was processed at the overpotential of 0.092 V vs RHE in the electrolyte (pH = 6), which was composed of hexamethylenetetramine ($C_6H_{12}N_4$, 0.30 M), potassium chloride (KCl, 0.20 M), and hydrochloric acid (HCl, 0.10 M) in water and $NiCl_2{\cdot}6H_2O$ (1.0×10^{-3} M) aqueous solution which mixed uniformly. For comparison, the electrolyte (pH = 6) containing hexamethylenetetramine ($C_6H_{12}N_4$, 0.30 M), potassium chloride (KCl, 0.20 M), and hydrochloric acid (HCl, 0.10 M) in water (without nickel ion) was also used. Prior to irradiation, the electrolyte was deaerated by bubbling gas mixture (80% N_2 and 20% CH_4) for 20 min. Methane was used as the internal standard for quantitative gas chromatograph analysis. The photocurrent density response was measured by chronoamperometry under on−off illumination cycles. And the current−voltage characteristics were measured by linear sweep voltammetry. The method of PEC H_2 evolution was bulk electrolysis with coulometry which records the accumulation of charge quantity and photocurrent in the process of the reaction. Faradaic efficiency was calculated using the following equation:

$$\text{Faradic efficiency (\%)} = [100 \times H_2 \text{ produced (mol)} \times 2 \times 96485\ (\text{C}\cdot\text{mol}^{-1})] / \text{charge passed during electrolysis (C)}$$

For assessing the stability of the NiO/QDs photocathode, experiments were carried out in air saturated electrolyte (0.10 M KCl) at the overpotential of 0.3 V vs Ag/AgCl.

RESULTS AND DISCUSSION

The absorption spectrum of MPA-CdTe QDs is shown in Figure. 1. It can be seen that the absorption peak of obtained

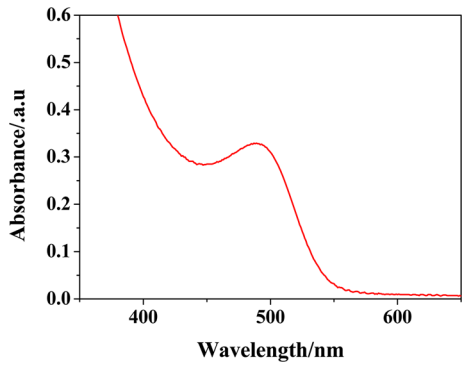

Figure 1. UV−vis absorption spectra of MPA-CdTe QDs.

sample at 490 nm is observed. And the diameter of MPA-CdTe QDs was estimated to be 2.04 nm by empiric formula.[25] MPA-CdTe QDs is adsorbed on a NiO film by covalent attachment through the carboxylic acid group.[14] For the NiO/QDs electrode, the photocurrent density was 26 $\mu A{\cdot}cm^{-2}$ and the dark current density was only 1.63 $\mu A{\cdot}cm^{-2}$, whereas little visible light response from the blank NiO electrode was observed under the same conditions (Figure. 2A). It is clear that the origin of the photocurrent lies in the excitation of MPA-CdTe QDs. From the current−voltage response of the NiO/QDs electrode ($J-V$ curves, Figure. 2B), the photocurrent density was remarkably higher than the dark current density. These results proved that MPA-CdTe QDs as a photosensitizer linked with the NiO film. And the adsorption of QDs was also demonstrated by scanning electron microscopy (SEM), which shows SEM images for unsensitized NiO sample and MPA-CdTe QDs sensitized NiO sample, respectively (Figure S1). Figure S1a shows the pristine NiO structures on the ITO substrate, which were grown as a porous honeycomb structure on the ITO surface. After the adsorption of CdTe, the surface of the NiO electrode became rugged as show in Figure S1b. The morphological changes of the NiO structure reveal that some QDs attached onto the surface of the NiO porous honeycomb structure. The surface compositions of the NiO/QDs electrode were determined by X-ray photoelectron spectroscopy (XPS). Figure S2a shows the scan survey spectra for the NiO/QDs electrode. The positions of Cd $3d_{3/2}$ and Cd $3d_{5/2}$ peaks for NiO/QDs electrode (Figure S2b) were at about 410.8 and 404.2 eV, which confirmed that Cd element existed mainly in the form of Cd^{2+} on the sample surface. Figure S2c shows the Te 3d peak, which presented the binding energies of Te $3d_{5/2}$ and Te $3d_{3/2}$ peaks at 572.6 and 583.1 eV, respectively. According to previous studies,[26] the Te 3d peak corresponds to Te−Cd bonds.

DOI: 10.1021/acssuschemeng.5b00450
ACS Sustainable Chem. Eng. 2015, 3, 2429−2434

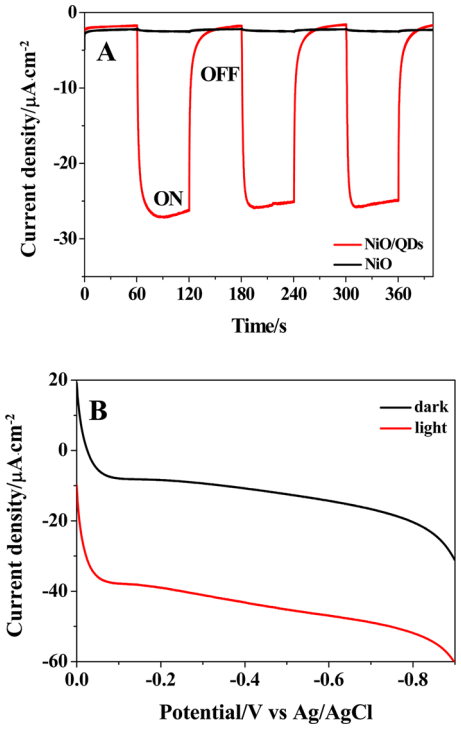

Figure 2. (A) Photocurrent density of blank NiO and NiO/QDs response to on−off cycles under light illumination at −0.222 V vs Ag/AgCl in an air saturated pH = 6.0 buffer solution; (B) current−voltage characteristics of NiO/QDs under illumination and dark in an air saturated pH = 6.0 buffer solution.

The high stability of photocathode should be important for the practical application of the PEC cell. To assess the stability of QD-sensitized photocathode, experiments were carried out in air saturated electrolyte (0.1 M KCl). The photocurrent kept stable over a 3 h illumination (Figure. 3). We also tested the

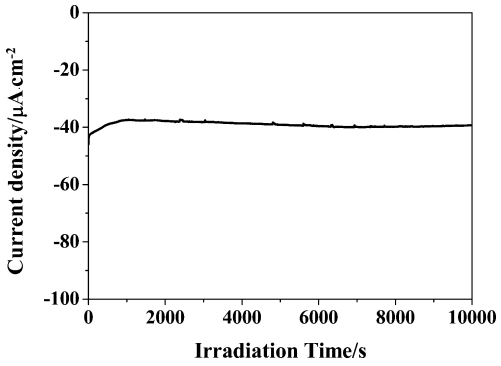

Figure 3. Current−time curves of NiO/QDs photocathode under light illumination at −0.3 V vs Ag/AgCl in air saturated electrolyte (0.10 M KCl).

stability for 20 times by $J-V$ curves. Within the scope of scanning from 0 to −0.9 V vs Ag/AgCl, the $J-V$ curves showed that the photocurrents had a little change that could be ignored (Figure S3). These results indicated that a stable photocathode was successfully fabricated.

Then, the photocathode was employed in a three-electrode and sealed PEC for H_2 evolution. Experimental results showed that the amount of H_2 evolution was 2.05 μmol, which was produced with 0.4 C of cathodic charge, corresponds to ∼100% Faradaic efficiency for 10 000 s of irradiation at the overpotential of 0.092 V.

To determine the factors that played the catalytic role in the experiment, a set of contrast experiments were carefully conducted. When the photocathode was not sensitized by MPA-CdTe QDs, only the NiO film was irradiated by a 300 W Xe lamp with a UV cutoff filter (λ > 400 nm) in a pH = 6.0 buffer solution with 1×10^{-3} M $NiCl_2{\cdot}6H_2O$. The unmodified NiO films showed small photocurrent response in the visible region (line a in Figure 5A), and no hydrogen was detected at −0.092 V vs RHE (Figure 4), confirming that the MPA-CdTe

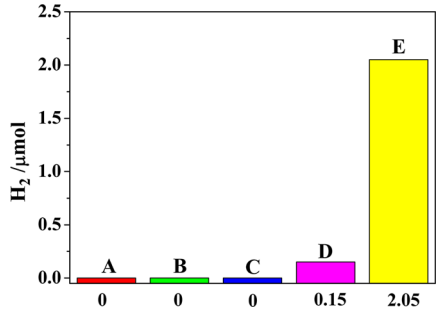

Figure 4. Comparison of the amount of H_2 evolution under different reaction conditions for 10 000 s. (A) NiO/QDs as working electrode in a pH = 6.0 buffer solution with 1×10^{-3} M $NiCl_2{\cdot}6H_2O$ under light illumination at 0 V vs RHE (without overpotential); (B) NiO/QDs as working electrode in a pH = 6.0 buffer solution with 1×10^{-3} M $NiCl_2{\cdot}6H_2O$ in the dark at −0.092 V vs RHE (without light); (C) NiO as working electrode in a pH = 6.0 buffer solution with 1×10^{-3} M $NiCl_2{\cdot}6H_2O$ under light illumination at −0.092 V vs RHE (without QDs); (D) NiO/QDs as working electrode in a pH = 6.0 buffer solution under light illumination at −0.092 V vs RHE (without Ni^{2+}); (E) NiO/QDs as working electrode in a pH = 6.0 buffer solution with 1×10^{-3} M $NiCl_2{\cdot}6H_2O$ under light illumination at −0.092 V vs RHE.

QDs are responsible for the hydrogen generation. When the photocathode was sensitized by MPA-CdTe QDs, the NiO/QDs photocathode was irradiated by a 300 W Xe lamp with a UV cutoff filter (λ > 400 nm) in a pH = 6.0 buffer solution and the photocurrent exhibited modest increase because QDs enhanced the efficiency of photon harvesting (line b in Figure 5A). And 0.15 μmol hydrogen, which was produced with 0.089 C of cathodic charge, corresponds to 32.5% Faradaic efficiency (Figure 4). However, when the photocathode was sensitized by MPA-CdTe QDs, the NiO/QDs photocathode was irradiated by a 300 W Xe-lamp with a UV cutoff filter (λ > 400 nm) in a pH = 6.0 buffer solution with 1×10^{-3} M $NiCl_2{\cdot}6H_2O$, the photocurrent showed substantial growth (line c in Figure 5A). And the hydrogen production quantity could reach 2.05 μmol, which increased almost 13 times than the buffer solution without $NiCl_2$ (Figure 4). These experiments indicated that both QDs and $NiCl_2$ are necessary to produce hydrogen by water splitting under visible light irradiation. Similarly, the $J-V$ curves also showed wide difference (Figure 5B). Then, other control experiments in the absence of either overpotential or visible light were conducted for hydrogen production by water splitting, and the results showed no hydrogen generated (Figure 4). So, QDs, nickel ion, overpotential, and visible light are all essential to produce hydrogen by water splitting.

To examine further the reproducibility and mechanism of the photocathode in the PEC, one continuous irradiation cycle was performed (Figure S4). During the course of the 60 000 s experiment, as high as 10.38 μmol H_2 was produced, which was

DOI: 10.1021/acssuschemeng.5b00450
ACS Sustainable Chem. Eng. 2015, 3, 2429−2434

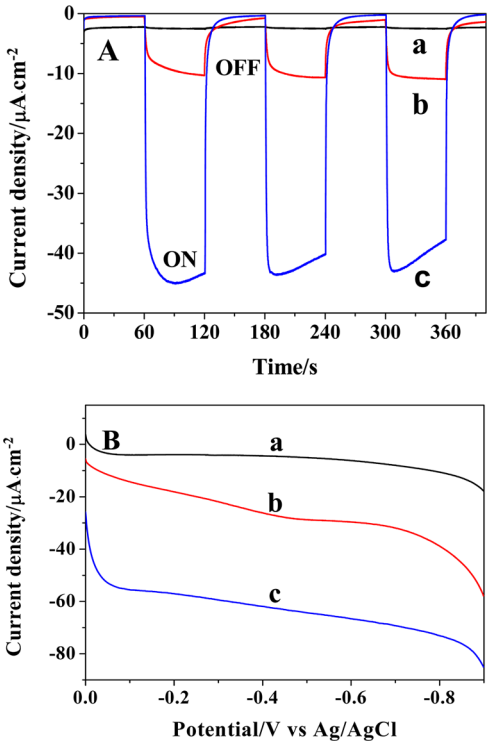

Figure 5. (A) Photocurrent density response to on−off cycles under light illumination at −0.222 V vs Ag/AgCl in a pH = 6.0 buffer solution; (B) current−voltage characteristics under light illumination for samples in a pH = 6.0 buffer solution. For both panels A and B, (a) NiO as working electrode in a pH = 6.0 buffer solution with 1×10^{-3} M $NiCl_2 \cdot 6H_2O$; (b) NiO/QDs as working electrode in a pH = 6.0 buffer solution; (c) NiO/QDs as working electrode in a pH = 6.0 buffer solution with 1×10^{-3} M $NiCl_2 \cdot 6H_2O$.

produced with 2.013 C of cathodic charge, and corresponds to 99.5% Faradaic efficiency (under irradiation 30 000 s). Although there is still no precise standard to compare the performance of reported PEC hydrogen evolution photocathodes because of the difference on photocathode materials and hydrogen generation conditions. According to the key parameters summarized in Table S1, it can be found that our photocathode was among the robust photocathodes for photoelectrochemical production of H_2.[12,13,15,27−32] When the 60 000 s experiment finished, the photocathode gradually turned from yellow to black. However, no change of the electrode color was observed in the control experiments without Ni^{2+}. From Figure S4, it is clearly observed that the kinetics of H_2 generation vary during the course of the experiment. The slopes of the three periods are different. Evidently, some reaction about nickel ion occurred on the surface of the NiO/QDs photocathode in the PEC process. Because of the sources of measurement error, such as the error in measuring the gas flow rate or the error in gas quantity measurement by the GC, there are little gaps between the actual value and theoretical value.

Recently, Z.-J. Li et al. have proposed that their artificial photocatalytic systems for H_2 evolution was formed by an in situ deposition of cobalt ion or nickel ion on QDs.[16,20] In this work, the black substance structure could also be a new composition, which is different from CdTe and NiO. To confirm this assumption, XPS of S and Ni on electrode were characterized in detail.

Before irradiation, the S 2p spectrum of the MPA-CdTe QDs could be well fit with one doublet with S $2p_{1/2}$ peaking at 162.85 eV and S $2p_{3/2}$ at 161.91 eV (Figure S5). These binding energies demonstrate the existence of chemical bonds between the thiols of MPA and the cadmium ions on the surface of the CdTe QDs. After irradiation, the S 2p doublet shifted to a lower binding energy, which suggests that illumination caused changes to the coordination situations for S from the MPA. A new doublet peak at 162.48 eV for S $2p_{1/2}$ and at 161.25 eV for S $2p_{3/2}$ implied that irradiation leads to the decomposition of MPA to CdS.[33] Thus, the photodecomposition process resulted in changes in the chemical properties of the photoelectrode.

Additionally, the Ni signals from the composition were detected (Figure S6). Because the metal ions can bind to the hanging bond (S^{2-}),[34] we speculated there would be a small amount of nickel ions present on the QDs. Really, before irradiation, the Ni 2p spectrum of NiO could be well fit with Ni $2p_{3/2}$ at 855.2 and 853.6 eV, which agrees well with the pattern of NiO.[35] After irradiation, a Ni $2p_{3/2}$ weak peak at ca. 853 eV[36] was observed, which demonstrated the existence of chemical bonds between the thiols of MPA and the Ni^{2+} from electrolyte. The high-resolution TEM micrograph of the composition is given in Figure S7, which supports the formation of NiS composition at QDs (NiS@QDs).

To determine further the exact chemical composition after irradiation, the XRD patterns of NiS@QDs are presented in Figure S8. As shown, the diffraction patterns of CdS (JCPDS Card No. 01-0647) and NiS (JCPDS Card No. 02-1443) were observed, corresponding to the HRTEM image, which supported the formation of NiS composition at QDs (NiS@QDs). Because of the aggregation of the CdTe QDs and the partial decomposition of MPA during illumination, the diffraction patterns of CdTe QDs was not detected, but the HRTEM image (Figure S7) supported that CdTe QDs were attached to the NiO films. The typical lattice plane distance of 3.52 Å is identical to that of CdTe QDs.

The accurate cognition of NiS@QDs composition will help us understand the mechanism in photoelectrocatalysis hydrogen evolution. The principle of NiO/QDs film as a photocathode for the water splitting reaction is presented in Scheme 1. When visible light is bombarded on the surface of NiO/QDs, the hole−electron pairs generate (eq 1.1). The holes in the valence band can be delivered to the NiO semiconductor through the carboxylic acid group, and consumed by the external circuit, which reduced the chance of electron−hole recombination. On the other hand, upon irradiation by visible light, the hanging bonds (S^{2-}) and the cadmium ions distributed on the surface of the QDs to form few CdS (eq 1.2), together with CdTe as photosensitizers. And the other hanging bonds (S^{2-}) coordinate with Ni^{2+} ions intimately to form NiS (eq 1.3) as the real catalytic unit NiS@QDs for H_2 generation. The photogenerated electrons in the conduction band of QDs can be easily transferred to the surface of NiS@QDs, which also prevents the recombination of electron−hole pairs of QDs. And then, the electron transfer from conduction band of QDs to the NiS@QDs results in the reduction of H^+ to H_2 (eq 1.4). The NiS that forms on the QDs surface during the PEC experiment enhances the kinetics of hydrogen generation. Just recently, NiS has been developed as an efficient cocatalyst for hydrogen evolution.[37−40] Excess Ni^{2+} ions in the solution would be helpful to avoid the dissociation of Ni^{2+} from the catalyst and to increase the working lifetime of the catalyst.

DOI: 10.1021/acssuschemeng.5b00450
ACS Sustainable Chem. Eng. 2015, 3, 2429−2434

Scheme 1. Illustration of the Working Principle of QDs Sensitized NiO Film as a Photocathode for Water Splitting Reaction under Visible Light Illumination

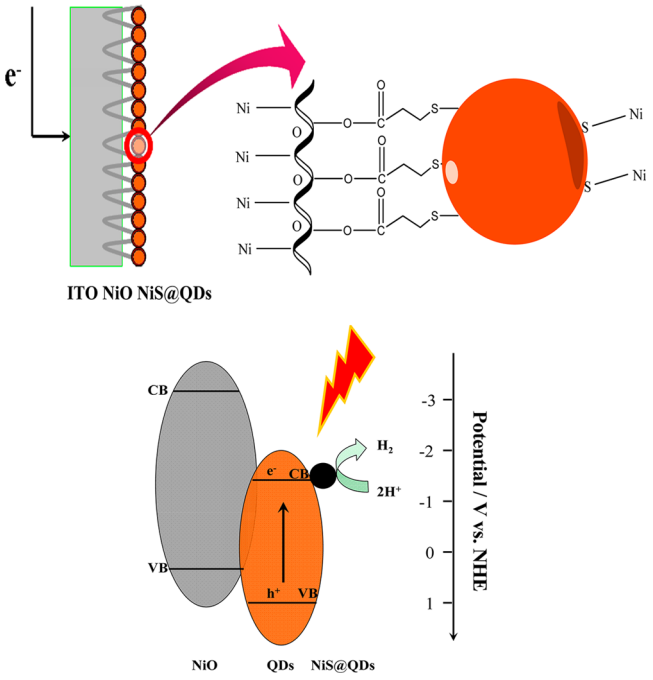

$$NiO/QDs + h\nu \rightarrow NiO/QDs\ (e_{CB}^{-} + h_{VB}^{+}) \quad (1.1)$$

$$Cd^{2+} + S^{2-} + h\nu \rightarrow CdS \quad (1.2)$$

$$Ni^{2+} + S^{2-} + h\nu \rightarrow NiS \quad (1.3)$$

$$e_{CB}^{-} + H^{+} \xrightarrow{NiS@QDs} 1/2H_2 \quad (1.4)$$

CONCLUSIONS

In summary, we demonstrated a robust and stable QDs-sensitized photocathode that sustained solar-driven hydrogen generation illuminated by visible light. At a low overpotential, the photocurrent response of the photocathode was steady over several hours and the performance of hydrogen generation achieved high efficiency, which corresponded to a Faradaic efficiency of almost 100%. The formation of NiS@QDs composition during illumination transferred the electron rapidly and enhanced the activity of hydrogen generation. This work has opened a promising way to developing efficient and durable photocathodes for PEC hydrogen generation and would pave the way toward the implementation of tandem solar cells.

ASSOCIATED CONTENT

Supporting Information

The Supporting Information is available free of charge on the ACS Publications website at DOI: 10.1021/acssuschemeng.5b00450.

SEM images of unsensitized NiO sample and MPA-CdTe QDs sensitized NiO sample, survey scan XPS spectrum, current−voltage characteristics under light illumination for NiO/QDs photocathode in air saturated electrolyte, time course of H_2 evolution with NiO/QDs/NiS@QDs under visible light irradiation, S 2p XPS spectra recorded from NiS@QDs composition and MPA-CdTe QDs, Ni 2p XPS spectra recorded from NiS@QDs composition and NiO, HRTEM images of NiS@QDs composition, XRD patterns of NiS@QDs composition, comparison of the performance of photocathodes (PDF).

AUTHOR INFORMATION

Corresponding Author

*Y. Dong. Fax: +86 510 85917763. E-mail: dongym@jiangnan.edu.cn.

Author Contributions

†These authors contributed equally to this work.

Notes

The authors declare no competing financial interest.

ACKNOWLEDGMENTS

We gratefully acknowledge the support from the National Natural Science Foundation of China (No. 20903048, 21275065), the Fundamental Research Funds for the Central Universities (JUSRP51314B), and MOE & SAFEA for the 111 Project (B13025).

REFERENCES

(1) Martin, D. J.; Qiu, K.; Shevlin, S. A.; Handoko, A. D.; Chen, X.; Guo, Z.; Tang, J. Highly Efficient Photocatalytic H_2 Evolution from Water using Visible Light and Structure-Controlled Graphitic Carbon Nitride. *Angew. Chem., Int. Ed.* **2014**, *53*, 9240−9245.

(2) Martin, D. J.; Reardon, P. J. T.; Moniz, S. J. A.; Tang, J. Visible Light-Driven Pure Water Splitting by a Nature-Inspired Organic Semiconductor-Based System. *J. Am. Chem. Soc.* **2014**, *136*, 12568−12571.

(3) Kenney, M. J.; Gong, M.; Li, Y.; Wu, J. Z.; Feng, J.; Lanza, M.; Dai, H. High-Performance Silicon Photoanodes Passivated with Ultrathin Nickel Films for Water Oxidation. *Science* **2013**, *342*, 836−840.

(4) Jacobsson, T. J.; Fjällström, V.; Edoff, M.; Edvinsson, T. Sustainable Solar Hydrogen Production: from Photoelectrochemical Cells to PV-Electrolyzers and Back Again. *Energy Environ. Sci.* **2014**, *7*, 2056−2070.

(5) Seger, B.; Laursen, A. B.; Vesborg, P. C. K.; Pedersen, T.; Hansen, O.; Dahl, S.; Chorkendorff, I. Hydrogen Production Using a Molybdenum Sulfide Catalyst on a Titanium-Protected n^+p-Silicon Photocathode. *Angew. Chem., Int. Ed.* **2012**, *51*, 9128−9131.

(6) Bourgeteau, T.; Tondelier, D.; Geffroy, B.; Brisse, R.; Laberty-Robert, C.; Campidelli, S.; de Bettignies, R.; Artero, V.; Palacin, S.; Jousselme, B. A H_2-Evolving Photocathode Based on Direct Sensitization of MoS_3 with an Organic Photovoltaic Cell. *Energy Environ. Sci.* **2013**, *6*, 2706−2713.

(7) Ding, Q.; Meng, F.; English, C. R.; Cabán-Acevedo, M.; Shearer, M. J.; Liang, D.; Daniel, A. S.; Hamers, R. J.; Jin, S. Efficient Photoelectrochemical Hydrogen Generation Using Heterostructures of Si and Chemically Exfoliated Metallic MoS_2. *J. Am. Chem. Soc.* **2014**, *136*, 8504−8507.

(8) Zang, G.-L.; Sheng, G.-P.; Shi, C.; Wang, Y.-K.; Li, W.-W.; Yu, H.-Q. A Bio-Photoelectrochemical Cell with a MoS_3-Modified Silicon Nanowire Photocathode for Hydrogen and Electricity Production. *Energy Environ. Sci.* **2014**, *7*, 3033−3039.

(9) Paracchino, A.; Laporte, V.; Sivula, K.; Gratzel, M.; Thimsen, E. Highly Active Oxide Photocathode for Photoelectrochemical Water Reduction. *Nat. Mater.* **2011**, *10*, 456−461.

(10) Zhang, Z.; Dua, R.; Zhang, L.; Zhu, H.; Zhang, H.; Wang, P. Carbon-Layer-Protected Cuprous Oxide Nanowire Arrays for Efficient Water Reduction. *ACS Nano* **2013**, *7*, 1709−1717.

(11) Morales-Guio, C. G.; Tilley, S. D.; Vrubel, H.; Grätzel, M.; Hu, X. Hydrogen Evolution from a Copper(I) Oxide Photocathode

DOI: 10.1021/acssuschemeng.5b00450
ACS Sustainable Chem. Eng. 2015, 3, 2429−2434

Coated with an Amorphous Molybdenum Sulphide Catalyst. *Nat. Commun.* **2014**, *5*, 3059.
(12) Tong, L.; Iwase, A.; Nattestad, A.; Bach, U.; Weidelener, M.; Götz, G.; Mishra, A.; Bäuerle, P.; Amal, R.; Wallace, G. G.; Mozer, A. J. Sustained Solar Hydrogen Generation Using a Dye-Sensitised NiO Photocathode/$BiVO_4$ Tandem Photo-electrochemical Device. *Energy Environ. Sci.* **2012**, *5*, 9472−9475.
(13) Ji, Z.; He, M.; Huang, Z.; Ozkan, U.; Wu, Y. Photostable p-Type Dye-Sensitized Photoelectrochemical Cells for Water Reduction. *J. Am. Chem. Soc.* **2013**, *135*, 11696−11699.
(14) Ji, Z.; Wu, Y. Photoinduced Electron Transfer Dynamics of Cyclometalated Ruthenium(II)−Naphthalenediimide Dyad at NiO Photocathode. *J. Phys. Chem. C* **2013**, *117*, 18315−18324.
(15) Li, L.; Duan, L. L.; Wen, F. Y.; Li, C.; Wang, M.; Hagfeldt, A.; Sun, L. C. Visible light driven hydrogen production from a photo-active cathode based on a molecular catalyst and organic dye-sensitized p-type nanostructured NiO. *Chem. Commun.* **2012**, *48*, 988−990.
(16) Li, Z.-J.; Li, X.-B.; Wang, J.-J.; Yu, S.; Li, C.-B.; Tung, C.-H.; Wu, L.-Z. A Robust "Artificial Catalyst" *in Situ* Formed from CdTe QDs and Inorganic Cobalt Salts for Photocatalytic Hydrogen Evolution. *Energy Environ. Sci.* **2013**, *6*, 465−469.
(17) Chen, H. M.; Chen, C. K.; Chang, Y.-C.; Tsai, C.-W.; Liu, R.-S.; Hu, S.-F.; Chang, W.-S.; Chen, K.-H. Quantum Dot Monolayer Sensitized ZnO Nanowire-Array Photoelectrodes: True Efficiency for Water Splitting. *Angew. Chem., Int. Ed.* **2010**, *49*, 5966−5969.
(18) Han, Z.; Qiu, F.; Eisenberg, R.; Holland, P. L.; Krauss, T. D. Robust Photogeneration of H_2 in Water Using Semiconductor Nanocrystals and a Nickel Catalyst. *Science* **2012**, *338*, 1321−1324.
(19) Han, Z.; Eisenberg, R. Fuel from Water: The Photochemical Generation of Hydrogen from Water. *Acc. Chem. Res.* **2014**, *47*, 2537−2544.
(20) Li, Z.-J.; Wang, J.-J.; Li, X.-B.; Fan, X.-B.; Meng, Q.-Y.; Feng, K.; Chen, B.; Tung, C.-H.; Wu, L.-Z. An Exceptional Artificial Photocatalyst, Ni_h-CdSe/CdS Core/Shell Hybrid, Made in Situ from CdSe Quantum Dots and Nickel Salts for Efficient Hydrogen Evolution. *Adv. Mater.* **2013**, *25*, 6613−6618.
(21) Li, Z.-J.; Fan, X.-B.; Li, X.-B.; Li, J.-X.; Ye, C.; Wang, J.-J.; Yu, S.; Li, C.-B.; Gao, Y.-J.; Meng, Q.-Y.; Tung, C.-H.; Wu, L.-Z. Visible Light Catalysis-Assisted Assembly of Ni_h-QD Hollow Nanospheres in Situ via Hydrogen Bubbles. *J. Am. Chem. Soc.* **2014**, *136*, 8261−8268.
(22) Wu, L.-Z.; Chen, B.; Li, Z.-J.; Tung, C.-H. Enhancement of the Efficiency of Photocatalytic Reduction of Protons to Hydrogen via Molecular Assembly. *Acc. Chem. Res.* **2014**, *47*, 2177−2185.
(23) Maeda, K.; Domen, K. Photocatalytic Water Splitting: Recent Progress and Future Challenges. *J. Phys. Chem. Lett.* **2010**, *1*, 2655−2661.
(24) Esswein, A. J.; Nocera, D. G. Hydrogen Production by Molecular Photocatalysis. *Chem. Rev.* **2007**, *107*, 4022−4047.
(25) Yu, W. W.; Qu, L.; Guo, W.; Peng, X. Experimental Determination of the Extinction Coefficient of CdTe, CdSe, and CdS Nanocrystals. *Chem. Mater.* **2003**, *15*, 2854−2860.
(26) Bartolo-Pérez, P.; Farías, M. H.; Castro-Rodríguez, R.; Peña, J. L.; Caballero-Briones, F.; Cauich, W. XPS analysis of oxidation states of Te in CdTe oxide films grown by rf sputtering with an Ar -NH_3 plasma. *Superficies Vacio.* **2001**, *12*, 8−11.
(27) Ruberu, T.; Dong, Y.; Das, A.; Eisenberg, R. Photo-electrochemical Generation of Hydrogen from Water Using a CdSe Quantum Dot-Sensitized Photocathode. *ACS Catal.* **2015**, *5*, 2255−2259.
(28) Yang, H. B.; Miao, J.; Hung, S.-F.; Huo, F.; Chen, H. M.; Liu, B. Stable Quantum Dot Photoelectrolysis Cell for Unassisted Visible Light Solar Water Splitting. *ACS Nano* **2014**, *8*, 10403−10413.
(29) Kumar, B.; Beyler, M.; Kubiak, C. P.; Ott, S. Photo-electrochemical Hydrogen Generation by an [FeFe] Hydrogenase Active Site Mimic at a *p*-Type Silicon/Molecular Electrocatalyst Junction. *Chem. - Eur. J.* **2012**, *18*, 1295−1298.
(30) Nann, T.; Ibrahim, S. K.; Woi, P. M.; Xu, S.; Ziegler, J.; Pickett, C. J. Water Splitting by Visible Light: A Nanophotocathode for Hydrogen Production. *Angew. Chem., Int. Ed.* **2010**, *49*, 1574−1577.
(31) Krawicz, A.; Yang, J.; Anzenberg, E.; Yano, J.; Sharp, I. D.; Moore, G. F. Photofunctional Construct That Interfaces Molecular Cobalt-Based Catalysts for H_2 Production to a Visible-Light-Absorbing Semiconductor. *J. Am. Chem. Soc.* **2013**, *135*, 11861−11868.
(32) Liu, B.; Li, X. B.; Gao, Y. J.; Li, Z. J.; Meng, Q. Y.; Tung, C. H.; Wu, L.-Z. A solution-processed, mercaptoacetic acid-engineered CdSe quantum dot photocathode for efficient hydrogen production under visible light irradiation. *Energy Environ. Sci.* **2015**, *8*, 1443−1449.
(33) Bao, H.; Gong, Y.; Li, Z.; Gao, M. Enhancement Effect of Illumination on the Photoluminescence of Water-Soluble CdTe Nanocrystals: Toward Highly Fluorescent CdTe/CdS Core−Shell Structure. *Chem. Mater.* **2004**, *16*, 3853−3859.
(34) Nag, A.; Chung, D. S.; Dolzhnikov, D. S.; Dimitrijevic, N. M.; Chattopadhyay, S.; Shibata, T.; Talapin, D. V. Effect of Metal Ions on Photoluminescence, Charge Transport, Magnetic and Catalytic Properties of All-Inorganic Colloidal Nanocrystals and Nanocrystal Solids. *J. Am. Chem. Soc.* **2012**, *134*, 13604−13615.
(35) Yang, Z. G.; Zhu, L. P.; Guo, Y. M.; Tian, W.; Ye, Z. Z.; Zhao, B. H. Valence-band offset of p-NiO/n-ZnO heterojunction measured by X-ray photoelectron spectroscopy. *Phys. Lett. A* **2011**, *375*, 1760−1763.
(36) Galtayries, A.; Grimblot, J. Formation and Electronic Properties of Oxide and Sulphide Films of Co, Ni and Mo Studied by XPS. *J. Electron Spectrosc. Relat. Phenom.* **1999**, *98*−*99*, 267−275.
(37) Chen, Z.; Sun, P.; Fan, B.; Zhang, Z.; Fang, X. In Situ Template-Free Ion-Exchange Process to Prepare Visible-Light Active g-C_3N_4/NiS Hybrid Photocatalysts with Enhanced Hydrogen Evolution Activity. *J. Phys. Chem. C* **2014**, *118*, 7801−7807.
(38) Geng, H.; Kong, S. F.; Wang, Y. NiS Nanorod-Assembled Nanoflowers Grown on Graphene: Morphology Evolution and Li-ion Storage Applications. *J. Mater. Chem. A* **2014**, *2*, 15152−15158.
(39) Wei, L.; Chen, Y.; Zhao, J.; Li, Z. Preparation of NiS/$ZnIn_2S_4$ as a Superior Photocatalyst for Hydrogen Evolution under Visible Light Irradiation. *Beilstein J. Nanotechnol.* **2013**, *4*, 949−955.
(40) Sun, X.; Dou, J.; Xie, F.; Li, Y.; Wei, M. One-step Preparation of Mirror-Like NiS Nanosheets on ITO for the Efficient Counter Electrode of Dye-Sensitized Solar Cells. *Chem. Commun.* **2014**, *50*, 9869−9871.

DOI: 10.1021/acssuschemeng.5b00450
ACS Sustainable Chem. Eng. 2015, 3, 2429−2434